Chapter 1

Introduction

1.1 Motivation

This thesis explores the reductive protonation of triply bonded small molecules, such as dinitrogen (N_2) and the cyanide anion (CN^-). Particularly critical is the reduction of N_2. All nitrogen in biomolecules is sourced from N_2, primarily through its industrial and biological reduction to ammonia (NH_3).[1] NH_3 also holds potential as a solar fuel due to its energy density and the availability of N_2.[2]

The industrial Haber-Bosch reaction, critical to synthetic fertilizer production, hydrogenates N_2 to NH_3.[1] This is a mildly exothermic reaction, but requires high temperatures and pressures, as well as a catalyst to activate kinetically inert N_2 (Figure 1.1). These reaction conditions are associated with high energy requirements and favor large, centralized NH_3 production. In addition, the H_2 for the Haber-Bosch process is sourced from steam reformation of methane, resulting in considerable CO_2 emissions.[1]

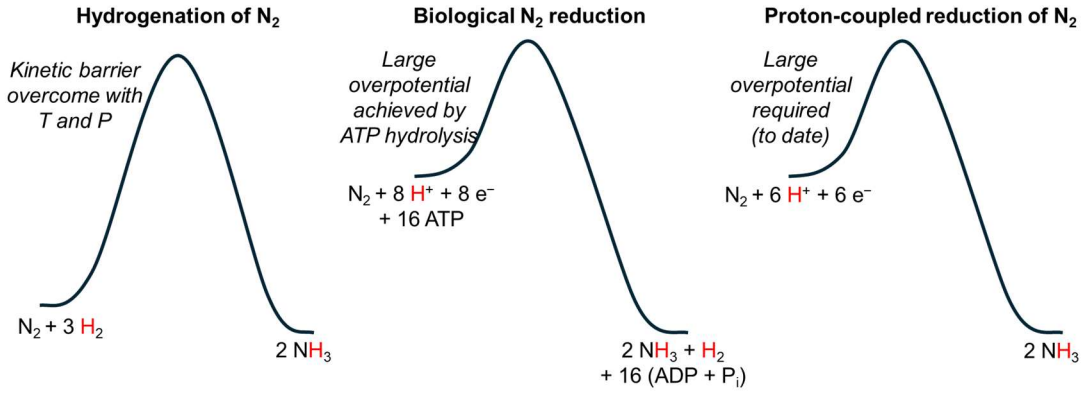

Figure 1.1. The energy input for industrial, biological, and chemically/electrochemically driven N_2R.

As an alternative, N_2 can be reductively protonated by $6H^+/6e^-$ at ambient conditions to yield NH_3 (nitrogen reduction, N_2R), with heterogeneous,[3] homogeneous,[4] and enzymatic[5] examples. However, to overcome the barriers associated with N_2 activation, examples of N_2R utilize a chemical overpotential − ATP hydrolysis in biological N_2R[6] or a highly cathodic overpotential or strong reductants in heterogeneously/homogeneously catalyzed N_2R (Figure 1.1).[4,7] The works discussed herein are directly or indirectly concerned with this overpotential. Two major topics are covered: the Fe-catalyzed chemical reduction of CN^-, a

reaction with interesting parallels to N_2R, and the development of photodriven N_2R and resulting photochemical insights. This introduction will provide context for these two topics and present some overarching themes.

1.2 Definitions relating to proton-coupled electron transfers

This thesis concerns proton-coupled reductions, a field that suffers from a variety of similar and ever-developing terms. It is therefore useful to define some phrases as I use and understand them.[8,9] A *proton-coupled reduction* (used interchangeably with *reductive protonation*) involves the addition of H^+/e^- to a substrate, forming X–H bonds during substrate reduction. Relevant to this thesis is the $6H^+/6e^-$ reduction of N_2 to 2 equivalents of NH_3 and the $7H^+/6e^-$ reduction of CN^- to yield CH_4 (methane) and NH_3. Both these transformations require a catalyst to activate the substrate, but the reagent(s) supplying H^+ and e^- are also critical.

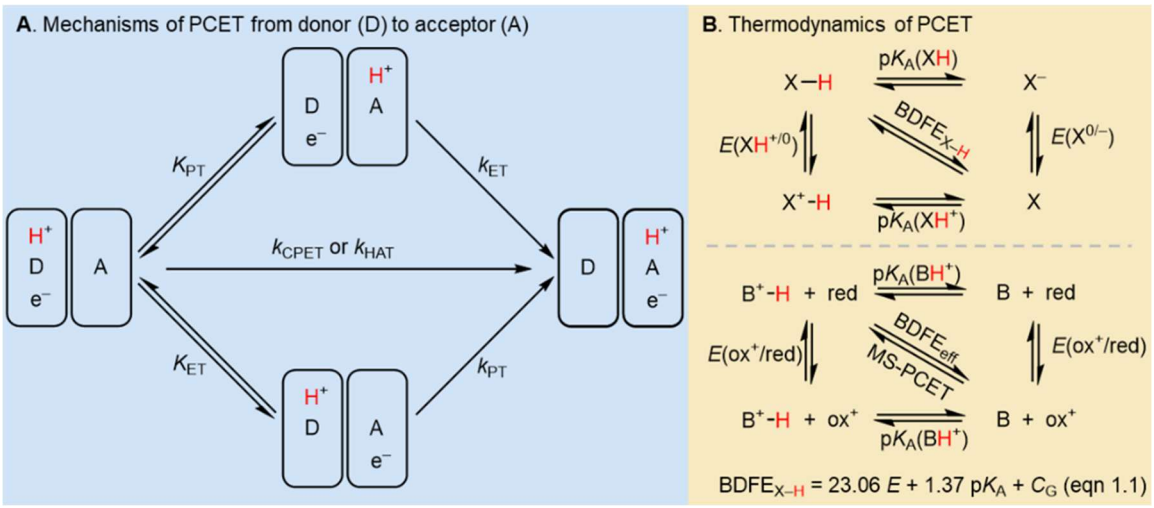

Figure 1.2. Mechanisms and thermodynamics of proton-coupled electron transfer.

Proton-coupled reductions might involve one or more *proton-coupled electron transfer* (PCET) steps. PCET implies that the transfer of a proton and an electron from a donor to an acceptor is kinetically or thermodynamically coupled. A PCET mechanism may still occur via sequential proton transfer (PT) and electron transfer (ET), e.g., via a pre-equilibrium (Figure 1.2A). If the PT and ET are kinetically coupled, we might designate the step as a concerted proton-electron transfer (CPET) or a hydrogen atom transfer (HAT). The

distinction lies in whether the H^+ and e^- are transferred to different orbitals (CPET) or the same orbital (HAT).[10]

An important mode of PCET reactivity is multisite-PCET (MS-PCET).[11,12] In the reductive direction, such reactions involve transferring the H^+ and e^- from different molecules to form one X−H bond. The entropic barrier associated with these termolecular steps often requires pre-coordination of one of the reagents, e.g., via H-bonding.

The thermodynamics of net $H^\bullet$ transfer between PCET reagents can be readily compared using the Bordwell equation (Figure 1.2B, eqn 1.1).[13,14] The inputs of reduction potential, acidity, and a solvent-dependent constant (C_G) allow us to calculate the bond dissociation free energy (BDFE) for a (net) HAT donor or a combination of reagents that perform MS-PCET (designated as effective BDFE; $BDFE_{eff}$). The $BDFE_{eff}$ values determined can be related to the thermodynamics of a proton-coupled reduction. For example, $BDFE_{eff}$ can be compared to $BDFE(H_2)_{H–H}$ or $BDFE(NH_3)_{N–H,\ ave}$ to assess the thermodynamics of hydrogen evolution reaction (HER) or N_2R, respectively.[7,15] Similarly, the $BDFE_{eff}$ can inform the kinetics of a reductive protonation. Simply stated, the weakest X−H bond formed during reductive protonation of a substrate is rarely much weaker than the $BDFE_{eff}$ supplied by reagent(s).[7,16] This basic principle can be used to rationalize and predict much of the reactivity discussed herein.

1.3 Biological Reductions of Dinitrogen and Cyanide

With this framework in place, we can introduce the proton-coupled reductions discussed in this thesis. Given our interest in modeling enzymatic reactivity to test and constrain mechanistic hypotheses, we first introduce the biological context for N_2 and CN^- reduction. Nitrogenase enzymes are the only class of enzymes known to reduce N_2 to NH_3.[5,6] This occurs at a metal-sulfur cluster active site, $[MFe_7S_9C]$ (M = V, Fe or Mo, abbreviated as [FeM]-cofactor; Figure 1.3 depicts the [FeMo]-cofactor, also know as FeMoco).[17] Two equivalents of NH_3 are generated, alongside one equivalent of H_2, with two ATP hydrolyzed per ET (i.e., 16 ATP are hydrolyzed per N_2 reduced, Figure 1.3). Nitrogenase enzymes are selective for NH_3 among N-fixed products, although the [VFe]-protein produces some hydrazine (N_2H_4; 4 e^- product).[18] Many parts of the mechanism of biological N_2R remain

poorly understood, such as the site(s) of N_2 binding, the six N−H bond formations, and the N−N bond cleavage step. However, the existence of [FeFe]-nitrogenases[19] and spectroscopic evidence from the heterometallic cofactors[20,21] suggest one or more Fe-sites play a key role in substrate binding and reduction.

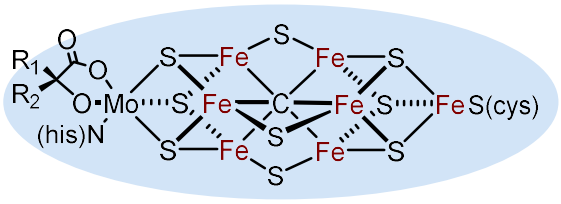

FeMo-cofactor - Active site of MoFe-protein

$N_2 + 8\,H^+ + 8\,e^- + 16\,ATP \xrightarrow[20\text{-}40\ ^\circ C]{\text{Nitrogenase}} 2\,NH_3 + H_2 + 16\,ADP$ (1 atm)

Ratio:N_2H_4/NH_3
MoFe protein: 0.0
VFe protein: 0.001-0.01

$HCN + 6\,H^+ + 6\,e^- + 12\,ATP \xrightarrow[25\ ^\circ C,\ 1\ atm\ Ar]{\text{Nitrogenase}} NH_3 + CH_4 + 12\,ADP$

Ratio: CH_3NH_2/CH_4
MoFe protein: 0.4
VFe protein: 0.6-1.1
Trace C_2H_4, C_2H_6 and CH_2NH

Figure 1.3. Comparison of N_2 reduction and HCN reduction at nitrogenase enzymes.

Interestingly, nitrogenases can reductively protonate several other substrates, including triply bonded small molecules like acetylene (HCCH),[22] carbon monoxide (CO),[23] methyl isocyanide (CNMe),[24,] and hydrogen cyanide (HCN).[25] Similar to N_2R, these reactions occur at the [FeM]-cofactor and require ATP to drive ET. HCN is reduced to primarily CH_4+NH_3 (6 e^- product) and methyl amine (CH_3NH_2; 4 e^- product), with methyl imine (CH_2NH; 2 e^- product) and trace C_2 products (ethane and ethylene) also detected (Figure 1.3).[16,26,27,28] Unlike the reduction of N_2, the coevolution of H_2 is not required. The isolobal analogy between substrate and products in cyanide and nitrogen reduction has motivated the mechanistic comparison of these two proton-coupled reductions.[29,30]

1.4 Catalytic N_2 reduction with well-defined molecular complexes

Well-defined molecular complexes, more amenable to spectroscopic studies and systematic variation, can also reduce N_2 to NH_3.[4,31] These systems can guide hypotheses

relating to substrate reduction at the nitrogenase active site and provide strategies for more efficient N_2R.

Building on studies of the protonation of terminal dinitrogen complexes ($M{-}N_2$; M = Mo or W) to yield NH_3,[32,33] Yandulov and Schrock demonstrated the first example of the catalytic reduction of N_2 to NH_3 with a well-defined molecular catalyst.[31,34] This first catalytic system used a (trisamidato)amine molybdenum ($(N_3N'Mo)$) precatalyst and decamethylchromocene (Cp^*_2Cr; $E_{1/2}(Cr^{III/II}) = -1.47$ V vs. $Fc^{+/0}$ in THF; all redox potentials are vs. $Fc^{+/0}$ in THF)[35] and 2,6-dimethylpyridinium ([LutH]BAr^F_4, pK_a 9.5 in THF, all pK_a in THF)[36] as the e^- and H^+ sources.

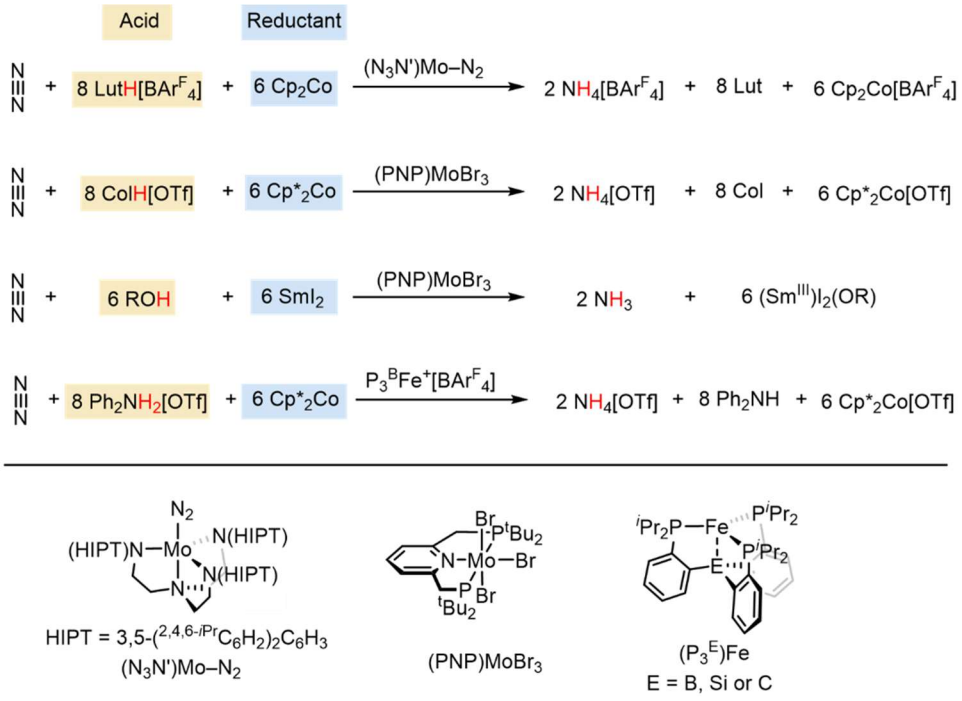

Figure 1.4. Conditions and catalysts for molecular catalytic N_2R critical to the work discussed in this thesis.

In 2011, Nishibayashi and coworkers introduced the bis(phosphino)pyridine pincer-molybdenum complex, $[((Mo)(N_2)_2)_2(\mu\text{-}N_2)]$ as a precatalyst for N_2R.[37] This first report used cobaltocene (Cp_2Co; $E_{1/2}(Co^{III/II}) = -1.33$ V) and LutH[OTf] as the e^-/H^+ source. Later it was shown that using trihalide precatalysts, $(PNP)Mo^{III}X_3$ (X = I or Br), and a more potent

reductant, decamethylcobaltocene (Cp^*_2Co; $E_{1/2}(Co^{III/II})$ = −1.97 V), and 2,4,6-trimethylpyridinium triflate ($[ColH]^+$; pK_a 10.4) acid, yields and rates improved.[38] Further improvements were achieved using SmI_2 ($E_{1/2}(Sm^{III/II})$ = −1.55 V) as a reductant and alcohol as the proton source (ROH, e.g., ethylene glycol).[39] These Sm-based reactions yield $Sm^{III}(OR)$ as the spent acid/reductant. Since this report, remarkable progress has been made in recovering such reagents[40] including a photochemical method presented in Chapter 6.

The proposed role of Fe in biological N_2R has motivated the study of Fe-catalyzed N_2R. The Peters group reported the first example of catalytic N_2R using an iron tris(phosphino)borane precatalyst (P_3^BFe) and initially with $[H(OEt_2)_2]BAr^F_4$ (pK_a < 0) and reductant KC_8 ($E(K^{0/+})$ <−3 V) as the H^+/e^- source.[41] Subsequent studies have shown that softer reagents, Cp^*_2Co and chlorinated anilinium triflates ($ArNH_3[OTf]$; pK_a 1.2 to 8.0, best yields with pK_a 4.3), showed improved yields.[42,43] Interestingly, the N-fixed products of Fe-catalyzed N_2R can be shifted from NH_3 to N_2H_4 by shifting the precatalyst,[44] acid/reductant choice,[45] or irradiation.[46]

Mechanistic experiments and the characterization of intermediates have allowed detailed mechanistic pictures to be built up for these described molecular systems. The Chatt cycles, initially used to describe stoichiometric N_2 protonations, have found significant utility in describing the Schrock group's Mo-catalyzed N_2R and the Fe-catalyzed systems described by the Peters group.[4,47] The Chatt cycles are monometallic pathways starting from terminal dinitrogen complexes (M−N≡N; Figure 1.5). In the Distal Chatt cycle, $3H^+/3e^-$ are first added to N_β, with N−N bond cleavage giving an equivalent of NH_3 and a metal nitride (M≡N). The nitride is then reductively protonated to yield a 2nd equivalent of NH_3. The Alternating Chatt cycle sequentially forms N_β−H and N_α−H bonds and can yield N_2H_4 from hydrazyl intermediates ($MN(H)NH_2$). However, evidence from both W and Fe complexes has shown that stoichiometric reactivity of the respective terminal hydrazido complexes ($M=N-NH_2$) can also yield N_2H_4.[32,48] It is proposed that N_α−H bond formation from the hydrazido yields the hydrazyl intermediate, allowing for N_2H_4 formation (this is designated as the Hybrid Distal-to-Alternating cycle). Therefore, hydrazidos are often the selectivity-determining intermediate in N_2R (at least for N-fixed products).

While hydrazidos are selectivity-determining intermediates, the overpotential of molecular N_2R via a Chatt cycle is proposed to be determined by the 1st N–H bond formation, i.e., to form the metal diazenido (M–N=N–H). In fact, there is often a close correlation between $BDFE_{N-H}$(M(NN–H)) and the $BDFE_{eff}$ of acid/reductant combinations used in the described catalytic reactions.[7]

Another pathway relevant to catalytic N_2R is the nitride splitting pathway. Access to a bimetallic dinitrogen complex allows splitting into two metal nitrides[49] that can be reductively protonated to yield NH_3 (Figure 1.5).[4] N_2R with (PNP)$MoBr_3$ precatalysts (Cp^*_2Co/ColH[OTf] or SmI_2/ROH as reactants) are thought to proceed through this mechanism via a [Mo^I–N≡N–Mo^I] intermediate.[50]

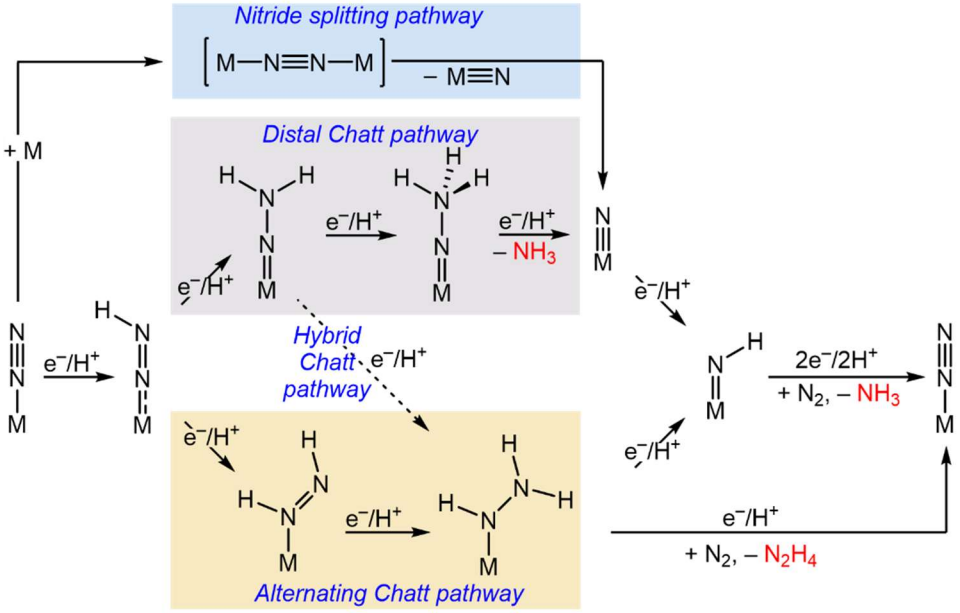

Figure 1.5. Mechanisms of catalytic N_2R at well-defined molecular complexes.

1.5 Cyanide Reduction

The role of HCN as a non-native substrate of nitrogenase has motivated the study of cyanide reduction. ATP-independent reductions of CN^- with extracted or synthetic Fe–S clusters have been reported using Eu^{II}(DTPA)/pH 8 buffer or SmI_2/[LutH]OTf as a reductant/acid.[51,52,53,54] These Fe–S cluster-catalyzed reactions yield substantial C_{2+} products

(~20%) regardless of the choice of precatalyst or conditions. While the observed C_{2+} products are undoubtedly interesting, this does suggest a mechanism that diverges from that observed by nitrogenase under ATP-dependent conditions. In addition, a lack of spectroscopic or mechanistic data has limited comparisons to N_2R. Electrochemical reduction and hydrogenation of HCN using heterogeneous catalysts have also been demonstrated.[55,56]

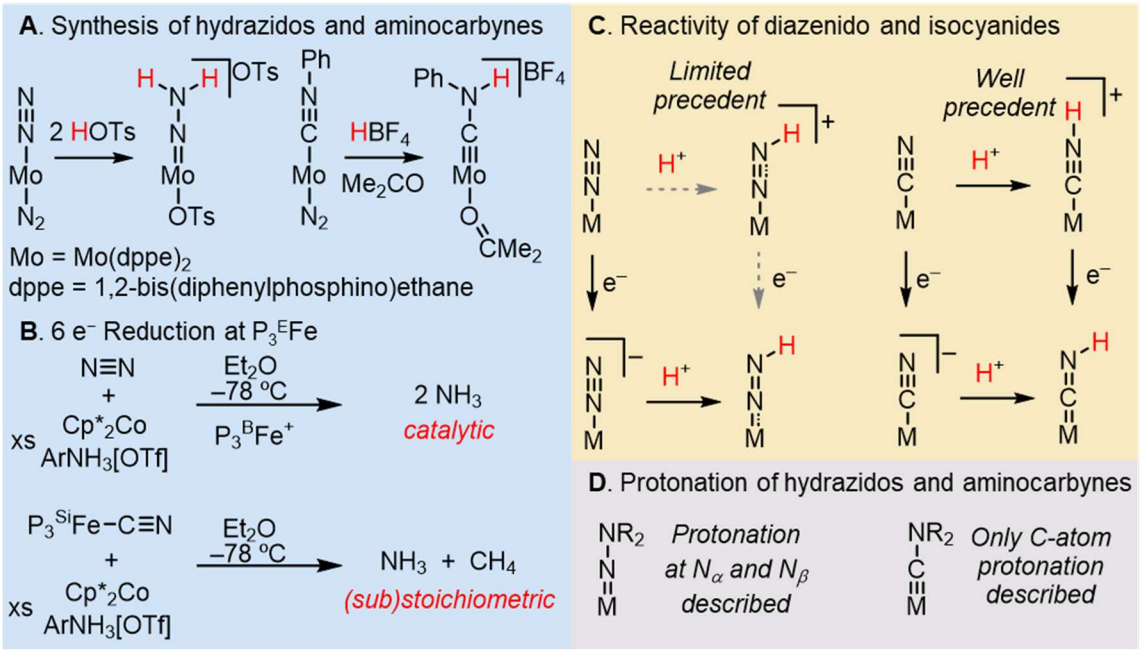

Figure 1.6. Comparison of molecular CN^- reduction and N_2R. $ArNH_3$ = $^{2,5\text{-Cl}}PhNH_2$.

Stoichiometric reductions of cyanide and isocyanide with well-defined molecular complexes have also been explored, often using the framework provided by the Chatt cycles.[57,58] The monoprotonation of d^6 alkyl and aryl isocyanide complexes yields aminocarbynes,[59,60,61,62] analogs of the hydrazidos invoked in N_2R (Figure 1.6A).[63] Further protonation of these complexes can yield primary amines, consistent with 6 e^- reduction of the isocyanide ligand. However, low amounts of CH_4 suggest hydrolysis is a considerable side reaction.[60,64,64] Our laboratory has previously shown stoichiometric CN^- reduction to CH_4 and NH_3 at a mononuclear Fe-complex with a tris(phosphino)sylil ligand (P_3^{Si}).[65] This reaction resembles the Fe-catalyzed N_2R with similar catalysts and reagent combinations (Figure 1.6B). Iron aminocarbynes were characterized and invoked as intermediates of this cyanide reduction.

With the molecular reduction of N_2 and CN^- introduced, we can highlight some key contrasts explored in Chapters 2 and 3. The CN^- ligand is more basic than N_2, with linear ($\angle$C−N−H ~ 180°) isocyanide geometries that maintain the C−N triple bond readily available (Figure 1.6C).[66] By contrast, the N_2 ligand requires greater activation before it can be protonated, with diazenido species typically featuring bent geometries and decreased N−N bonding. These differences might allow for different mechanisms of early N−H bond formation.

Following early N−H bond formation, the differing reactivity of hydrazidos and aminocarbynes might provide interesting contrasts. As noted, transition metal hydrazidos often determine selectivity for NH_3 or N_2H_4 via N_β or N_α−H bond formation, with catalytic and stoichiometric evidence for both reactivity patterns.[33,48**Error! Bookmark not defined.**,67,68,69] By contrast, examples of aminocarbyne protonation exclusively show C−H bonds to yield aminocarbenes,[70,71,72] an interesting observation in light of the selectivity for CH_4 and NH_3 observed in many CN^- reduction reactions (Figure 1.6D). However, discussions of the frequently observed selectivity for CH_4 and NH_3 were lacking in the literature.

1.6 Photodriven N_2R: Motivation and approach

As noted, N_2R requires an energy input, which, under ambient conditions with molecular catalysts, is supplied by a chemical overpotential from strong reductants and/or acids (Figure 1.1). How to lower this overpotential is a fascinating question that has motivated a lot of beautiful chemistry, and I would direct readers to some of the chemistry developed in parallel with my own thesis work.[73,74] However, zooming out, it is striking that despite considerable improvements in turnover number, utility, rate, and selectivity, the overpotential for chemical N_2R has not improved in 20 years. This motivated the exploration of alternate methods to generate high overpotentials.

An alternate approach to achieve large chemical overpotentials with otherwise mild reagents is to use light as the additional energy input. While small molecule activations such as hydrogen evolution,[75] CO_2 reduction (CO_2R),[76] and water oxidation[77] have received considerable attention, such an approach had not previously been disclosed in the molecular N_2R literature. Proposed examples of photodriven N_2R with semiconductors, including in

concert with nitrogenase, have been reported, but low yields and/or high amounts of non-N_2 derived NH_3 remain issues.[78,79,80,81]

Upon excitation by a photon, the reducing power of a photoreductant or photocatalyst increases, allowing it to be the strong reductant required for N_2R. Based on this principle, we envisioned a chemical system for which a dark reaction has an overpotential for N_2R close to 0, but upon irradiation, sufficient driving force is generated by photogenerated reductants (Figure 1.7C, left panel). Such a system might provide a thermodynamic analog of the Haber-Bosch reaction, but instead of temperature and pressure, the reaction would be driven by light.

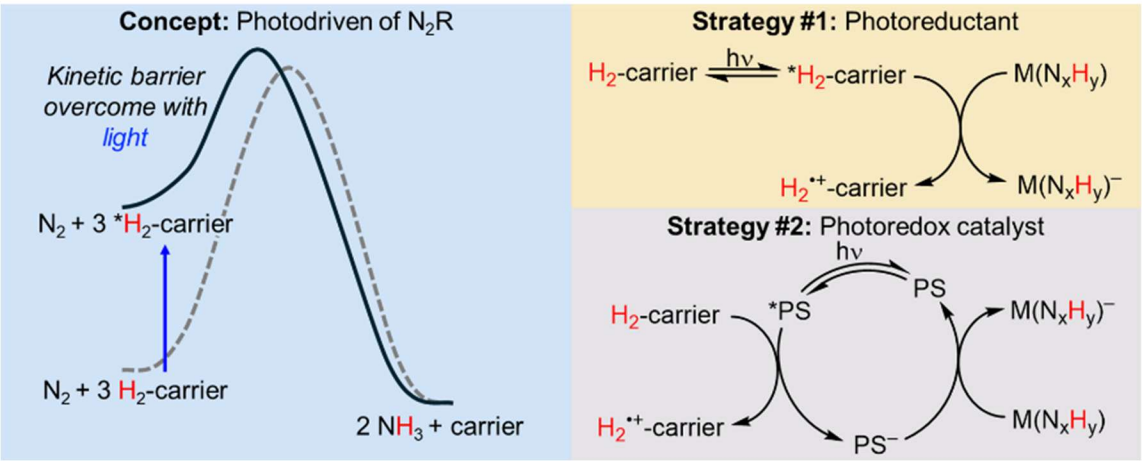

Figure 1.7. Concept for photodriven N_2R with molecular complexes. The overpotential required for N_2R with molecular catalysts is supplied by excitation; two strategies are shown.

Ideally, H_2 could be used directly, but while there are examples of photoactivation of H_2 or N_2, integration into catalytic N_2R cycles remains challenging.[82,83,84] As an alternative, H_2-carriers, reagents with labile H-atoms with a comparable overpotential for hydrogenation to H_2 can be used.[85,86] Such reagents can be directly photoexcited[87,88] or used in conjugation with a photoredox catalyst.[89,90] Unlike alkyl amines, common reductive quenchers in photodriven CO_2R or HER, H_2-carriers allow a large pK_a window for added buffers or acids, desirable attributes for N_2R, where a low pK_a is often required. In addition, clean oxidation of the carrier would allow for careful thermodynamic analysis.

The challenge then becomes how to, upon irradiation, convert the H^+/e^- stored in the H_2-carrier into reagents competent for the proton-coupled reduction of N_2. Using conditions for thermal N_2R as a guide, we envisioned two strategies in which the H_2-carrier might be activated to reduce N_2R intermediates (generalized as $M(N_xH_y)$). A photoactive H_2-carrier could directly reduce $M(N_xH_y)$ from the excited state (Figure 1.7, Strategy 1). Examples of such systems being employed in photodriven small molecule reductions are limited, but photooxidants, particularly quinones, have found use in water oxidation.[91,92,93] Alternatively, an explicit photosensitizer could be used (Strategy 2). Following excitation, the photosensitizer can then be reduced by the H_2-carrier to generate a persistent reduced photosensitizer. ET from the reduced photosensitizer to $M(N_xH_y)$, in net transfers e^- from the H_2-carrier. In both strategies, the oxidized H_2-carrier is a potent donor for $2H^+/e^-$ allowing for further ET and PT steps in N_2R.[94,95] The inclusion of a buffer was posited to help facilitate these PT steps.

1.7 Hantzsch ester photoreductions

In short, both strategies worked, although the photoreductant strategy operates by a mechanism quite different from what we first envisioned. Attempting to understand this mechanism motivated investigations into the photochemistry of a specific H_2-carrier, the Hantzsch ester (HEH_2; Figure 1.8A), and given its importance in the latter half of this thesis, a short introduction is warranted.

HEH_2 is a dihydropyridine, similar to biological energy carriers like NADH. It was first synthesized in 1881[96] and has been known as a photoreductant for over 60 years.[87,97,98] The capabilities and limitations of the excited state of HEH_2 ($*HEH_2$) can be summarized in two key photophysical properties (Figure 1.8B): the excited state reduction potential, $E(HEH_2^{\bullet+}/*HEH_2) = -2.5$ V and excited state lifetime, $\tau_{1/2} = 200$ ps.[99] $*HEH_2$ will reduce many substrates, but the short, excited state lifetime limits diffusional reactivity. Therefore, $*HEH_2$ will reduce substrates that can pre-associate HEH_2 in the ground state (Figure 1.8C). π-stacked electron donor-acceptor (EDA) complexes are the most common mode by which such interactions have been described, utilized both in the reduction of simple organic

compounds and to activate R•-donors such as Katritzky salts ([$^{2,4,6\text{-Ph}}$PyrR]BF_4)[100] and *N*-hydroxyphthalimide esters.[101,102]

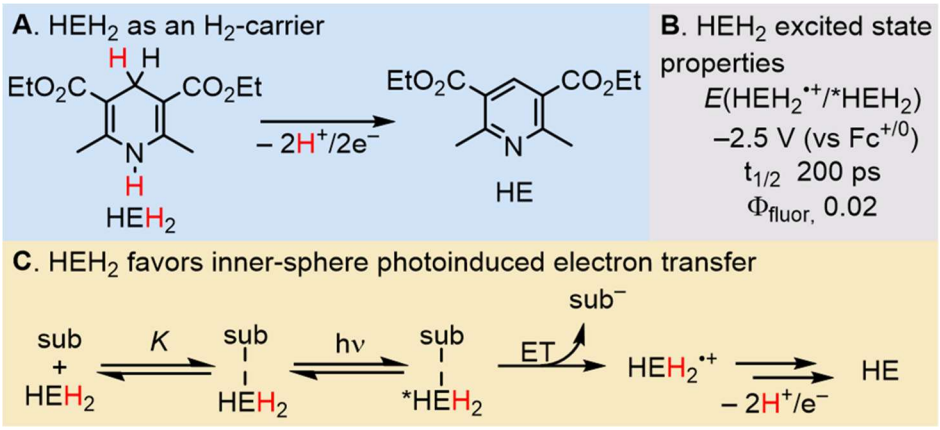

Figure 1.8. Key parameters of Hantzsch ester photoreactivity and potential utilization in selective reduction of substrates.

A question that arises when exploring HEH_2 photochemistry is the potential utility.[88] Are these photocatalyst-free reactions mere curiosities, or might they offer advantages beyond saving a few mol% precious metal photocatalysts? The short lifetime of *HEH_2 might provide a potential avenue by which one can achieve selectivity in photoreductions. Unlike long-lived or persistent photocatalysts, HEH_2 photoreductions require pre-association of the oxidant. This could allow for selective reductions in a pool of potential redox partners if one of them more strongly pre-associates to HEH_2. This motivates the further exploration of HEH_2 photochemistry beyond its application in N_2R, particularly understanding modes of pre-interaction and subsequent photoinduced electron-transfer steps.

1.8 Overview of the individual chapters

In **Chapter 2,** we developed conditions for the catalytic reduction of CN^- to CH_4 and NH_3 with high selectivity at a mononuclear Fe-site, $P_3^{Si}Fe$ using excess reductant ($(C_6H_6)_2Cr$; $E(Cr^{+/0}) = -1.22$ V) and acid ($Ph_2NH_2[OTf]$) to supply the required $7H^+/6e^-$. Following this discovery, we explored the mechanism of this reduction reaction, finding that terminal iron aminocarbynes ($P_3^{Si}FeCNH_2$) and iron aminocarbenes ($P_3^{Si}FeC(H)(NH_2)]^+$) as likely

intermediates. This mechanism is then compared to CN^- reduction at Fe−S clusters and N_2R at tris(phosphino)iron complexes, emphasizing the high selectivity for CH_4 and NH_3.

In **Chapter 3,** the initial steps of catalytic CN^- reduction, the $2H^+/2e^-$ conversion of $P_3^{Si}FeCN$ to $P_3^{Si}FeCNH_2$, are examined in detail. We demonstrate that these species can interconvert reversibly, an unusual observation in small-molecule triple bond reductions. The reductive reaction is studied over a wider range of conditions, with the previously measured thermochemistry of early N−H bonds of the iron cyanide platform found to be powerful predictors of reactivity. In addition, we analyze the kinetics of iron cyanide reduction to the iron aminocarbyne, finding that H-bonding to iron cyanide is key to a low barrier transformation. Finally, we evaluate factors enabling reversibility and discuss implications for lowering the driving force in Fe-catalyzed N_2R.

In **Chapter 4,** we develop conditions for the blue-light-driven reduction of N_2 to NH_3 using (PNP)$MoBr_3$ as a catalyst, HEH_2 as the H_2-donor, and Col-buffer. Unusually for a photodriven reduction reaction, an explicit photocatalyst was not required to observe N_2R. Still, the inclusion of an Ir-photocatalyst ($[Ir(ppy)_2(dtbbpy)]BAr^F_4$) boosted yields and rates. Under either set of conditions, the conversion of HEH_2 to the $2H^+/2e^-$ oxidized form, HE, allows for careful assessment of the thermodynamic effects of irradiation and suggests the possibility of photoreductant recovery/recycling. These conditions were also found to be competent for the reduction of nitrate to ammonia and acetylene to ethylene (with trace ethane).

Given the unusual efficiency of photodriven N_2R in the absence of a photocatalyst, in **Chapter 5**, we investigate the mechanism of this reaction further, focusing on the interaction of HEH_2 and Col-buffer. Through spectroscopic study, a detailed mechanism for the activation of HEH_2 by Col-buffer is proposed. In short, we observe H-bonding between HEH_2 and $[ColH]^+$ in the ground state. $[ColH]^+$ readily quenches $*HEH_2$, via a static quenching pathway, proposed as ET between the pre-associated species. Transient absorbance and EPR data suggest the base plays a critical role, rapidly deprotonating $HEH_2^{\bullet+}$. This results in the (net) formation of two potent H-atom donors, $ColH^\bullet$ and $HEH^\bullet$, with the

reduction of organic substrates used to benchmark their reactivity. Finally, some lessons for the photoreactivity of HEH_2 are discussed.

Finally, in **Chapter 6**, given the importance of SmI_2 as a selective one-electron reducing reagent for organic and inorganic reactions motivates the development of methods for Sm^{III} regeneration. However, photochemical methods illustrated to date were limited. Using lessons from Chapters 4 and 5, we developed conditions for the reduction of Sm^{III} precursors to SmI_2 via both a photoreductant approach with HEH_2 and a photoredox approach using HEH_2 as a reductive quencher with a photocatalyst, $[Ir(ppy)_2(dtbbpy)]PF_6$. Subsequently, we developed a proof-of-concept catalytic Sm-mediated ketone-acrylate coupling reaction.

1.9 Cited References

1. Smil, V. Enriching the Earth: Fritz Haber, Carl Bosch, and the Transformation of World Food Production; MIT Press: Cambridge, MA, USA, 2000.
2. Valera-Medina, A.; Xiao, H.; Owen-Jones, M.; David, W. I. F.; Bowen, P. J. *Prog. Energy Combust. Sci.* **2018**. 69, 63–102. .
3. Suryanto, B. H. R.; Matuszek, K.; Choi, J.; Hodgetts, R. Y.; Du, H.-L.; Bakker, J. M.; Kang, C. S. M.; Cherepanov, P. V.; Simonov, A. N.; MacFarlane, D. R. *Science* **2021**. 372, 1187. .
4. Chalkley, M. J.; Drover, M. W.; Peters, J. C. *Chem. Rev.* **2020**. 120, 5582–5636.
5. Seefeldt, L. C.; Yang, Z.-Y.; Lukoyanov, D. A.; Harris, D. F.; Dean, D. R.; Raugei, S.; Hoffman, B. M. *Chem. Rev*. **2020**. 120, 5082–5106.
6. Seefeldt, L. C.; Hoffman, B. M.; Peters, J. W.; Raugei, S.; Beratan, D. N.; Antony, E.; Dean, D. R. *Acc. Chem. Res.* **2018**. 51, 2179–2186.
7. Chalkley, M. J.; Peters, J. C. *Eur. J. Inorg. Chem*. **2020**. 2020, 1353–1357.
8. These terminologies largely align with those used in the following review, although this review uses *Concerted electron-proton transfer* (CEPT) instead of CPET.

Concerted-PCET is also used to describe the same phenomena. Ugh! Tyburski, R.; Liu, T.; Glover, S. D.; Hammarström, L. *J. Am. Chem. Soc.* **2021**. 143, 560–576.

9. While the discussions here focus on reductive PCET steps the same considerations can be applied to oxidative PCET steps.
10. Mayer, J. M.; Hrovat, D. A.; Thomas, J. L.; Borden, W. T. *J. Am. Chem. Soc.* **2002**. 124, 11142–11147.
11. Waidmann, C. R.; Miller, A. J. M.; Ng, C.-W. A.; Scheuermann, M. L.; Porter, T. R.; Tronic, T. A.; Mayer, J. M. *Energy Environ. Sci.* **2012**, 5, 7771–7780.
12. Morris, W. D.; Mayer, J. M. *J. Am. Chem. Soc.* **2017**. 139, 10312–10319.
13. Bordwell, F. G.; Cheng, J. Pei.; Harrelson, J. A. *J. Am. Chem. Soc.* **1988**. 110, 1229–1231.
14. Agarwal, R. G.; Coste, S. C.; Groff, B. D.; Heuer, A. M.; Noh, H.; Parada, G. A.; Wise, C. F.; Nichols, E. M.; Warren, J. J.; Mayer, J. M. *Chem. Rev.* **2022**. 122, 1–49.
15. Lindley, B. M.; Appel, A. M.; Krogh-Jespersen, K.; Mayer, J. M.; Miller, A. J. M. *ACS Energy Lett.* **2016**. 1, 698–704.
16. Gentry, E. C.; Knowles, R. R. *Acc. Chem. Res.* **2016**. 49, 1546–1556.
17. Einsle, O.; Rees, D. C. *Chem. Rev.* **2020**. 120, 4969–5004.
18. Dilworth, M. J.; Eady, R. R. *Biochem. J.* **1991**. 277, 465–468.
19. Chisnell, J. R.; Premakumar, R.; Bishop, P. E. *J. Bacteriol.* **1988**. 170, 27–33.
20. Spatzal, T.; Perez, K. A.; Einsle, O.; Howard, J. B.; Rees, D. C. *Science* **2014**. 345, 1620–1623.
21. Harris, D. F.; Lukoyanov, D. A.; Kallas, H.; Trncik, C.; Yang, Z.-Y.; Compton, P.; Kelleher, N.; Einsle, O.; Dean, D. R.; Hoffman, B. M.; Seefeldt, L. C. *Biochemistry* **2019**. 58, 3293–3301.
22. Lee, C. C.; Hu, Y.; Ribbe, M. W. *Science* **2010**. 329, 642–642.
23. Dilworth, M.J. *Biochim. Biophys. Acta BBA - Gen. Subj.* **1966**. 127, 285–294.
24. Rubinson, J. F.; Corbin, J. L.; Burgess, B. K. *Biochemistry* **1983**. 22, 6260–6268.

25. Kelly, M.; Postgate, J. R.; Richards, R. L. *Biochem. J.* **1967**. 102, 1-3C.
26. Li, J.; Burgess, B. K.; Corbin, J. L. *Biochemistry* **1982**. 21, 4393–4402.
27. Lowe, D. J.; Fisher, K.; Thorneley, R. N. F.; Vaughn, S. A.; Burgess, B. K. *Biochemistry* **1989**. 28, 8460–8466.
28. Fisher, K.; Dilworth, M. J.; Newton, W. E. *Biochemistry* **2006**. 45, 4190–4198.
29. Burgess, B. K.; Lowe, D. J. *Chem. Rev.* **1996**. 96, 2983–3012.
30. Pombeiro, A. J. L.; Richards, R. L. *Coord. Chem. Rev.* **1990**. 104 , 13–38.
31. Yandulov, D. V.; Schrock, R. R. *Science* **2003**. 301, 76–78.
32. Chatt, J.; Pearman, A. J.; Richards, R. L. *J. Chem. Soc.-Dalton Trans.* **1977**. 19, 1852–1860.
33. Anderson, S. N.; Fakley, M. E.; Richards, R. L.; Chatt, J. *J. Chem. Soc. Dalton Trans.* **1981**. 9, 1973–1980.
34. Schrock, R. R. *Acc. Chem. Res.* **2005**. 38, 955–962.
35. Connelly, N. G.; Geiger, W. E. *Chem. Rev.* **1996**. 96, 877–910.
36. Garrido, G.; Rosés, M.; Ràfols, C.; Bosch, E. *J. Solut. Chem.* **2008**. 37, 689–700. .
37. Arashiba, K.; Miyake, Y.; Nishibayashi, Y. *Nat. Chem.* **2011**. 3, 120–125.
38. Arashiba, K.; Eizawa, A.; Tanaka, H.; Nakajima, K.; Yoshizawa, K.; Nishibayashi, Y. *Bull. Chem. Soc. Jpn.* **2017**. 90, 1111–1118.
39. Ashida, Y.; Arashiba, K.; Nakajima, K.; Nishibayashi, Y. *Nature* **2019**. 568, 536–540.
40. The chemical and electrochemical recovery of $Sm^{III}I_2(OR)$ is an interesting topic that colleagues have made exceptional progress in the last few years, see: Boyd, E. A.; Shin, C.; Charboneau, D. J.; Peters, J. C.; Reisman, S. E. *Science* **2024**. 385, 847–853.
41. Anderson, J. S.; Rittle, J.; Peters, J. C. *Nature* **2013**. 501, 84–87.
42. Chalkley, M. J.; Del Castillo, T. J.; Matson, B. D.; Roddy, J. P.; Peters, J. C. *ACS Cent. Sci.* **2017**. 3, 217–223. .

43. Chalkley, M. J.; Del Castillo, T. J.; Matson, B. D.; Peters, J. C. *J. Am. Chem. Soc.* **2018**. 140, 6122–6129.
44. Hill, P. J.; Doyle, L. R.; Crawford, A. D.; Myers, W. K.; Ashley, A. E. *J. Am. Chem. Soc.* **2016**. 138, 13521–13524.
45. Boyd, E. A.; Peters, J. C. *J. Am. Chem. Soc.* **2023**. 145, 14784–14792.
46. Garrido-Barros, P.; Chalkley, M. J.; Peters, J. C. *Angew. Chem. Int. Ed.* **2023**. 62, e202216693.
47. Pickett, C. J. *J. Biol. Inorg. Chem.* **1996**. 1, 601–606.
48. Rittle, J.; Peters, J. C. *J. Am. Chem. Soc.* **2016**. 138, 4243–4248.
49. Laplaza, C. E.; Cummins, C. C. *Science* **1995**. 268, 861–863.
50. Bruch, Q. J.; Malakar, S.; Goldman, A. S.; Miller, A. J. M. *Inorg. Chem.* **2022**. 61, 2307–2318.
51. Lee, C. C.; Hu, Y.; Ribbe, M. W. *Angew. Chem. Int. Ed Engl.* **2012**. 51, 1947–1949.
52. Lee, C. C.; Hu, Y.; Ribbe, M. W. *Proc. Natl. Acad. Sci.* **2012**. 109, 6922–6926.
53. Tanifuji, K.; Lee, C. C.; Ohki, Y.; Tatsumi, K.; Hu, Y. L.; Ribbe, M. W. *Angew. Chem.-Int. Ed.* **2015**. 54, 14022–14025.
54. Tanifuji, K.; Sickerman, N.; Lee, C. C.; Nagasawa, T.; Miyazaki, K.; Ohki, Y.; Tatsumi, K.; Hu, Y.; Ribbe, M. W. *Angew. Chem. Int. Ed.* **2016**. 55, 15633–15636.
55. Debus, H. *J. Chem. Soc.* **1863**. 16, 249–260.
56. Fedurco, M.; Sartoretti, C. J.; Augustynski, J. *J. Am. Chem. Soc.* **1999**. 121, 888–889.
57. Pombeiro, A. J. L.; Guedes da Silva, M. F. C.; Michelin, R. A. *Coord. Chem. Rev.* **2001**. 218, 43–74.
58. By contrast examples of bimetallic CN^- cleavage (in analogy to the nitride splitting mechanism) have yet to be reported, see the following reference for a valiant effort: Peters, J. C.; Baraldo, L. M.; Baker, T. A.; Johnson, A. R.; Cummins, C. C. *J. Organomet. Chem.* **1999**, 591, 24–35.
59. Pombeiro, A. J. L.; Richards, R. L. *Transit. Met. Chem.* **1980**. 5, 281–284.

60. Chatt, J.; L. Pombeiro, A. J.; L. Richards, R. *J. Chem. Soc. Dalton Trans.* **1980**. 3, 492–498.
61. Seino, H.; Nonokawa, D.; Nakamura, G.; Mizobe, Y.; Hidai, M. *Organometallics* **2000**. 19, 2002–2011.
62. Hughes, D. L. ; Mohammed, M. Y.; Pickett, C. J. *J. Chem. Soc. Chem. Commun.* **1989**. 18, 1399–1400.
63. Chatt, J.; Leigh, G. J. *Chem. Soc. Rev.* **1972**, 1, 121–144.
64. Carvalho, M. F. N. N.; Pombeiro, A. J. L.; Schubert, U.; Orama, O.; Pickett, C. J.; Richards, R. L. *J. Chem. Soc. Dalton Trans*. **1985**. 10, 2079–2084.
65. Rittle, J.; Peters, J. C. *Angew. Chem. Int. Ed.* **2016**. 55, 12262–12265.
66. Pombeiro, A. J. L. *Inorg. Chem. Commun.* **2001**. 4, 585–597.
67. Galindo, A.; Hills, A.; Hughes, D. L.; Richards, R. L. *J. Chem. Soc. Chem. Commun.* **1987**. 24, 1815–1816. .
68. Glassman, T. E.; Vale, M. G.; Schrock, R. R. *J. Am. Chem. Soc.* **1992**, 114, 8098–8109.
69. Thompson, N. B.; Green, M. T.; Peters, J. C. *J. Am. Chem. Soc.* **2017**. 139, 15312–15315.
70. Filippou, A. C.; Wössner, D.; Lungwitz, B.; Kociok-Köhn, G. *Angew. Chem. Int. Ed. Engl.* **1996**, 35, 876–878.
71. Filippou, A. C.; Lungwitz, B.; Kociok-Köhn, G. *Eur. J. Inorg. Chem.* **1999**. 1999, 1905–1910. .
72. Cook, D. J.; Hill, A. F. *Organometallics* **1997**, 16, 5616–5617.
73. Garrido-Barros, P.; Derosa, J.; Chalkley, M. J.; Peters, J. C. *Nature* **2022**. 609, 71–76.
74. Boyd, E. A.; Jung, H.; Peters, J. C. *J. Am. Chem. Soc.* **2025**. 147, 4695–4700.
75. Esswein, A. J.; Nocera, D. G. *Chem. Rev.* **2007**, 107, 4022–4047.

76. Yamazaki, Y.; Takeda, H.; Ishitani, O. *J. Photochem. Photobiol. C Photochem. Rev.* **2015**. 25, 106–137.
77. Bofill, R.; García-Antón, J.; Escriche, L.; Sala, X. *J. Photochem. Photobiol. B* **2015**. 152, 71–81.
78. Brown, K. A.; Harris, D. F.; Wilker, M. B.; Rasmussen, A.; Khadka, N.; Hamby, H.; Keable, S.; Dukovic, G.; Peters, J. W.; Seefeldt, L. C.; King, P. W. *Science* **2016**. 352, 448–450.
79. Brown, K. A.; Ruzicka, J.; Kallas, H.; Chica, B.; Mulder, D. W.; Peters, J. W.; Seefeldt, L. C.; Dukovic, G.; King, P. W. *ACS Catal.* **2020**. 10, 11147–11152.
80. Schrauzer, G. N.; Guth, T. D. *J. Am. Chem. Soc.* **1977**, 99, 7189–7193.
81. Edwards, J. G.; Davies, J. A.; Boucher, D. L.; Mennad, A. *Angew. Chem. Int. Ed. Engl.* **1992**, 31, 480–482. .
82. Park, Y.; Kim, S.; Tian, L.; Zhong, H.; Scholes, G. D.; Chirik, P. J. *Nat. Chem.* **2021**. 13, 969–976.
83. Kim, S.; Park, Y.; Kim, J.; Pabst, T. P.; Chirik, P. J. *Nat. Synth.* **2022**. 1, 297–303.
84. Forrest, S. J. K.; Schluschaß, B.; Yuzik-Klimova, E. Y.; Schneider, S. *Chem. Rev.* **2021**. 121, 6522–6587.
85. Chen, M.-W.; Wu, B.; Liu, Z.; Zhou, Y.-G. *Acc. Chem. Res.* **2023**. 56, 2096–2109 .
86. Wang, D.; Astruc, D. *Chem. Rev.* **2015**. 115, 6621–6686.
87. Kurz, J. L.; Hutton, R.; Westheimer, F. H. *J. Am. Chem. Soc.* **1961**. 83, 584–588.
88. Crisenza, G. E. M.; Mazzarella, D.; Melchiorre, P. *J. Am. Chem. Soc.* **2020**. 142, 5461–5476.
89. Wang, P.-Z.; Chen, J.-R.; Xiao, W.-J. *Org. Biomol. Chem.* **2019**. 17, 6936–6951.
90. Prier, C. K.; Rankic, D. A.; MacMillan, D. W. C. *Chem. Rev.* **2013**, 113, 5322–5363.
91. Awad, M. K.; Anderson, A. B. *J. Am. Chem. Soc.* **1989**. 111, 802–806.
92. Hong, Y. H.; Jung, J.; Nakagawa, T.; Sharma, N.; Lee, Y.-M.; Nam, W.; Fukuzumi, S. *J. Am. Chem. Soc.* **2019**, 141, 6748–6754.

93. Hong, Y. H.; Lee, Y.-M.; Nam, W.; Fukuzumi, S. *J. Am. Chem. Soc.* **2022**, 144, 695–700. .
94. Shen, G.-B.; Fu, Y.-H.; Zhu, X.-Q. *J. Org. Chem.* **2020**. 85, 12535–12543.
95. Schmittel, M.; Burghart, A. *Angew. Chem. Int. Ed.* **1997**. 36, 2550–2589.
96. Hantzsch, A. *Berichte Dtsch. Chem. Ges.* **1881**, 14, 1637–1638.
97. Ohnishi, Y.; Kagami, M.; Ohno, A. *Chem. Lett.* **1975**, 4, 125–128.
98. Suresh Yedase, G.; Venugopal, S.; P., A.; Reddy Yatham, V. *Asian Journal of Organic Chemistry* **2022**. 11, e202200478.
99. Jung, J.; Kim, J.; Park, G.; You, Y.; Cho, E. J. *Adv. Synth. Catal.* **2016**. 358, 74–80.
100. Wu, J.; Grant, P. S.; Li, X.; Noble, A.; Aggarwal, V. K. *Angew. Chem. Int. Ed.* **2019**. 58, 5697–5701.
101. Kammer, L. M.; Badir, S. O.; Hu, R.-M.; Molander, G. A. *Chem. Sci.* **2021**. 12, 5450–5457.
102. Li, J.; Siang Tan, S.; Kyne, S. H.; Wai Hong Chan, P. *Adv. Synth. Catal.* **2022**. 364, 802–810.